Decay of the Ar $2p^5nd$ core resonances: An autoionization spectrum dominated by shake processes

M. Meyer, E. v. Raven, and B. Sonntag
II. Institut für Experimentalphysik, Universität Hamburg, Luruper Chaussee 149, D-2000 Hamburg, West Germany

J. E. Hansen
Zeeman Laboratory, University of Amsterdam, Plantage Muidergracht 4, NL-1018 TV Amsterdam, The Netherlands
(Received 7 May 1990)

The autoionization of the Ar $2p^5nd$ resonances has been studied both experimentally and theoretically. The effect of the partial collapse of the $3d$ wave function between the initial and the final state has been investigated with regard to shake probabilities as well as to the structure of the final ionic configuration. The decay probabilities depend strongly on the principal quantum number both of the core-excited Ar* $2p^5nd$ state and of the Ar^+ $3p^4n'd$ final state. One of the most striking features is that the $2p^5nd \rightarrow 3p^4nd\epsilon l$ decay is almost completely forbidden for $n=4$.

I. INTRODUCTION

The influence of correlation on the excitation and decay of the Xe $4d$-np, Kr $3d$-np, and Ar $2p$-ns,nd core resonances has been studied in a number of recent investigations (Refs. 1–6 and references therein). For atomic Ar the energy region of the $2p$ excitations is well known from absorption,[7] ion yield,[8] and energy-loss[9,10] spectra. There are also a number of experimental and theoretical studies of the *LMM* Auger spectrum (e.g., Refs. 11–15). However, in comparison to the situation for Xe and Kr the knowledge about the decay channels of the Ar $2p^5ns$ and nd inner-shell resonances, in particular, those leading to Ar^+ $3p^4ns$ and $3p^4nd$ final states, is rather limited. This is partly because the cross sections for selective excitations of Ar $2p$ electrons are very low[8] at the first resonance maximum; only 1.8 Mb, compared to the cross sections for Xe $4d$ and Kr $3d$ excitations which are about 14.2 and 7.5 Mb, respectively, at the lowest resonance maximum. The low cross sections in association with the higher photon energy makes the measurements rather difficult. The first investigation of the electron spectra emitted upon the decay of the Ar $2p$ resonances[3] demonstrated the importance of the collapse of the $3d$ wave function in the Ar^+ state, which causes an anomalously high intensity of the Ar* $2p^5(^2P_{3/2})\ 3s^23p^63d \rightarrow Ar^+$ $2p^63s^23p^44d\epsilon l$ shake-up satellites. However, it was difficult to analyze the data due to the many overlapping lines and Aksela *et al.*[16] have later noted that high-resolution measurements are needed to distinguish clearly between shake-up and main peaks. This is one of the motivations behind the present work. In addition, the $3p$-$3d$ interaction was not taken into account in the early work. This interaction results for the Ar^+ $3p^43d$ configuration in a multiplet structure[17] very different from that of the Ar^{2+} $3p^4$ configuration populated by the $L_{23}M_{23}M_{23}$ Auger decay. In addition, the $3p$-$3d$ interaction can cause a complex intensity distribution in the autoionization spectra as demonstrated for the Ca $2p^53d$ resonances.[18] For the Ar $2p^53d$ resonances we expect a smaller, but by no means negligible, $3p$-$3d$ interaction which will influence both the excitation and more importantly the decay. This fact further complicates the analysis of the decay pattern.

Heimann *et al.*[4] measured the spectrum of threshold electrons for photon energies close to the $2p$ ionization limits. They found very low intensities of threshold electrons at the energies corresponding to the first two resonances, but considerable threshold intensities for a number of unresolved higher resonances in the region of $n=6$ followed by a minimum leading up to the lowest $2p$ ionization limit. Heimann *et al.* ascribed this production of threshold electrons to shake-off decays, e.g., $2p^53d \rightarrow 3p^4\epsilon l\epsilon' l$, of the core resonances. This interpretation was supported by model calculations of the total shake probability including shake-up to discrete levels as well as shake-off to the continuum, but without distinguishing between the two processes. Based on their data it was hard to assess the importance of the two-step autoionization process which had been invoked by Hayaishi *et al.*[8] to explain the formation of Ar^{2+} ions below the $2p$ ionization limits. Recently, Hayaishi *et al.*[19] studied the relative yield spectra of Ar^{2+} and Ar^{3+} ions obtained in coincidence with threshold electrons. They demonstrated that those experimental facts, which cannot be explained by the shake-off model, can be accounted for by two-step autoionization decays such as $2p^55d \rightarrow 3p^46d\epsilon l \rightarrow 3p^4\epsilon l\epsilon l'$.

Recently the angular distribution of the electrons emitted upon the decay of the Ar $2p^5nl$ core resonances has been studied experimentally[5] and theoretically.[6]

Shake-up and shake-off processes are one aspect of electron correlation. Other aspects have also been studied. The autoionizing decay of the type of excited state in question has in a single-electron model been described by the "spectator model," which in brief assumes that the decay of the inner-shell hole is largely unaffected by the presence of the outer excited electron (see, for example,

Refs. 3 and 4). This model does not, therefore, allow for the occurrence of shake processes. Other types of deviations from the spectator model have been found also. For example, deviations observed in high-resolution experiments on the Ar* $2p^5 4s$ resonances could be explained by taking the *p-s* interaction into account.[20,21] However, as mentioned, the knowledge about the decay of the $2p^5 nd$ resonances is much less complete. In particular, the interplay between shake processes and the interaction of the partly collapsed $3d$ orbital with the $3p$ orbital has not been studied. In order to put our understanding of the model system Ar on more solid ground, we undertook a thorough experimental and theoretical investigation of the Ar* $2p^5(^2P_{3/2})3d$ and Ar* $2p^5(^2P_{3/2})4d$ resonances in which we have tried to understand the effects of the $3d$ collapse on both the shake processes as well as on the structure of the ion.

II. EXPERIMENT

The photoelectron spectra were measured at the FLIPPER I–wiggler–undulator beam line at the Hamburger Synchrotronstrahlungslabor (HASYLAB).[22] The atomic beam of high-purity Ar gas (99.99%) crossed the monochromatized synchrotron radiation in the source volume of a cylindrical mirror analyzer (CMA), which was used to determine the energy of the photoelectrons. Because the CMA accepts only electrons emitted close to the magic angle of 54°44′, with respect to the polarization vector of the light, the recorded photoelectron spectra are not affected by angular distribution effects. The electrons were retarded by a constant electric field in order to improve the kinetic-energy resolution which is given by the expression $\Delta E_{\rm kin}=0.01(E_{\rm kin}-eU_{\rm ret})$. The bandwidth of the monochromator was set to $\Delta\hbar\omega=0.6$ eV. Such good resolution is a prerequisite for the detailed comparison with theory which is presented in this paper.

III. THEORY

A. Shake probabilities

In principle, the theory of shake-up and -down processes is simple in that it consists of postulating that the electron leaves the atom so quickly that the initial-state wave function has no time to relax adiabatically and that, therefore, the probability that the atom will be found in a particular state after the ionization can be determined by projecting the initial wave function on the final states in the (relaxed) ion.[23] In practice, since in most cases the relaxation is small, the accuracy of the projection approach can be low since both initial- and final-state wave functions normally will have inaccuracies which can be as large as the relaxation effects.[24] In particular, correlation can be much more important than the change in potential if, for example, the electrons involved come from the same shell.[25] In the present case Aksela *et al.*[3] have published $2p^5 3s^2 3p^6 3d$ and $2p^6 3s^2 3p^4 3d$ and $4d$ wave functions, which show that the $3d$ orbital in Ar I (with one $2p$ hole present) has a much larger spatial overlap with the $4d$ than with the $3d$ orbital in Ar II (when two $3p$ holes are present). Thus it can be expected that the simplest form of the shake-up theory will give a more accurate result in this case than in more marginal cases. This expectation is borne out by the results which we will present here.

In order to obtain the shake probabilities we have calculated Hartree-Fock (HF) wave functions for the mean energy of the $2p^5 3s^2 3p^6 nd$ and $2p^6 3s^2 3p^4 nd$ configurations using the relativistic HF approximation due to Cowan and Griffin[26] and determined the overlap between the nd orbitals. The squares of the overlap factors are given as calculated branching ratios in Table I. To calculate branching ratios, in principle, requires that the overlaps with all final d states, bound and continuum, are calculated and the sum normalized to 100. However, for the initial $3d$, $4d$, $5d$, and $6d$ states, the sum over the final states with $n=3$–9 gives a total of more than 99.3 and for $3d$ and $4d$ the overlaps with $8d$ and $9d$ is less than 0.001. Thus we give squared overlaps without additional normalization, in other words neglecting the small probabilities of shake-up and shake-off to higher d states. This is in disagreement with the assumptions of Heimann *et al.*,[4] who assume that shake-off is important, but apparently not in disagreement with their actual, less extensive, calculations which seem to agree with our results (see below). In the spectator model, the initial $2p^5 4d$ state, for example, can decay to only one of the $3p^4 nd$ final configurations, namely $3p^4 4d$. Decay to $3p^4 n'd$ ($n'\neq 4$) becomes possible when shake-up or -down is considered. The numbers in Table I show for the initial $2p^5 4d$ state that 12% of the decay is predicted to go down to $2p^6 3s^2 3p^4 3d$ and 63% to go up to the $5d$ configuration, while the predicted intensity going to the $2p^6 3s^2 3p^4 4d$ final configuration is practically zero. This is a very unusual result for which no precedent is known

TABLE I. Observed and calculated intensities for the decay channels Ar* $2p^5 3s^2 3p^6 n'd \rightarrow Ar^+ 2p^6 3s^2 3p^4 nd$.

Initial state Ar*	Intensity of final states (%) $3p^4 nd$ $n=3$ expt.	$n=3$ calc.	$n=4$ expt.	$n=4$ calc.	$n=5$ expt.	$n=5$ calc.	$n=6$ expt.	$n=6$ calc.	$n=7$ expt.	$n=7$ calc.
$2p^5 3d$	43	32	47	60	10	5.8		0.004		0.003
$2p^5 4d$	13	12	<15	0.04	>40	63	32	24		0.2
$2p^5 5d$		6		0.8		8.0		32		50
$2p^5 6d$		3		0.7		1.7		13		4.7

to us and it seemed well worthwhile to try to verify this prediction experimentally. In order to do that high-resolution measurements were even more necessary than for the $2p^53d$ decay, as we will show.

As discussed already this approach to shake-up is very simple. However, there are a number of additional approximations in the approach we have used. As mentioned the HF calculations are for the mean energies of the configurations in question. HF calculations for the $p^5d\,^1P$ states can give rather different orbitals from those for the mean energy if the exchange interaction is large[27] and this is particularly important here because the ^1P state is the only one which has a dipole moment connecting it with the ground state. In the present case, $2p^53d$, exchange is less important than for $3p^53d$ and the effect is probably not too serious. Similarly, since the $3p^4nd$ final states are spread over a fairly large energy region (determined in the case of $n>3$ by the splitting of the parent configuration $3p^4$) there can also be some differences in the final-state orbitals between the highest and lowest levels. Also these differences have not been considered here. A further approximation has been made by only considering the overlap between the d orbitals while orbitals such as $3s$ and, in particular, $3p$ can be expected to relax somewhat also. There is, in addition, another process, which experimentally will manifest itself in the same way as a shake process but in reality is due to the interaction in the final ionic state. It will be described in the following section.

B. Auger decay

The other part of the calculation is the determination of the detailed Auger rates for the $2p^5nd$ excited states. The basic procedure is similar to that employed for the determination of the Auger decay of the $2p^54s^23d$ state in Ca (Ref. 18) although the only final configurations included here are $2p^63s^23p^4nl$ and $2p^63s3p^6$. These configurations are expected to be the most important on the basis of the Ca calculations. It is not possible to describe the interaction between $3s3p^6$ and the individual $3p^4nd$ configurations correctly if only one $3p^4d$ configuration is included,[28] but the error does nearly exclusively affect the $3p^4(^1D)d\,^2S$ term and is, therefore, not so important for the overall reliability of the results. In the excited state we have included the configurations $2p^53s^23p^6(4s+5s+6s+7s+3d+4d+5d)$ and in the final state $3s3p^6$ and $3s^23p^4(3d+4s+5s)$ for the calculation of the main lines in the case of the $3d$ resonance. For the calculation of the $3d$ "satellites," say, the final configurations were $3s3p^6$ and $3s^23p^4$ $(4d+5s+6s)$, $(5d+6s+7s)$, and $(6d+7s+8s)$, respectively. For the calculation of the satellites the Auger interaction integrals between the initial d state and the "normal" final continuum state (same principal d quantum number as in the excited state) were retained while the correct Slater integrals within the final $d+s$ configurations were used to give the structure of these configurations and the interaction between them. The reason that we have to repeat the calculations for each individual configuration instead of just applying the branching ratio from Table I to the results for the "main" feature is, of course, the large difference between the coupling conditions, in particular, between $3p^43d$ and the higher nd configurations. (On the other hand the main difference between the $2p^53d\rightarrow 3p^4nl$ and $2p^54d\rightarrow 3p^4nl$ decays are due to the differences in the initial-state couplings. Since the spin-orbit interaction of the $2p$ electron is the most important interaction in all the initial states, these differences are not so large.) The $s\rightarrow s'$ shake-up probability is set to zero and the calculation does, therefore, not describe the s satellites. In principle, the Auger interaction integrals depend on the energy of the free (continuum) electron. We have not included this effect in the calculation of the satellite intensities. We have used fixed core HF calculations for the average configuration energy to determine the continuum wave functions. However, the continuum electron energies are large and do not change very much in relative terms between different final states. Thus the effect resulting from the neglect of the energy dependence of the continuum wave functions is expected to be small. Because the continuum electron energies are large the importance of the coupling between the different continuum channels are also expected to be small and has likewise been neglected. Both assumptions appear to be justified from the good agreement obtained with experiment as described later.

In the calculation of the Auger interaction integrals, the overlap between the nd functions were set equal to 1 so that finally the branching ratios from Table I must be applied to give the relative strengths of the transitions to the different final $3p^4nd$ configurations. Decay to the $3p^4nd$ states due to both p and f waves were calculated. In the case of Ca we omitted the f wave[18] and in the case of the decay of the $2p$ hole in Ar Pan and Kelly report[29] that the probability for the $2p^53s^23p^6\rightarrow 2p^63s^23p^4$ decay via a p wave is 70.5%, while the probability for decay via an f wave is only 3.2%. Auger decays to $3s3p^5$ and $3s^03p^6$ final states account for 26.3% in their calculation. Although the p wave is the dominant one, we have, nevertheless, included the f wave for the decay of the $2p^5nd$ states. The comparison with the experimental results discussed later show that calculations at the few percent level are necessary in order to take advantage of the experimental accuracy. For Ca, where other final states are important also, we did not include the f wave since it would lead to very large calculations and the comparison with experiment did not show that the observed disagreements could be explained by the neglect of the f wave. In LS coupling some of the $3p^4nd$ levels built on $3p^4(^1D)$ can only be reached with an f wave and levels with $J>\frac{5}{2}$ cannot be reached at all with a p wave from the initial $2p^5nl$ states (see Table II). The decay to $3p^4(^1D)nd\,^2G$ is possible only with the f wave, and the fact that the ^2G state is observed in the experimental results demonstrates the need for including the f wave. Our results show, for the $3p^4(^1D)3d\,^2F$ term, that the f wave is nearly as important as the p wave for one of the three initial states but otherwise the f wave is important at the few percent level only, except for the $(^1D)\,^2G$ term.

We have, on the other hand, neglected the series interaction between the different $3p^4nd$ configurations. The nondiagonal electrostatic integrals connecting the dou-

blet terms built on different parent states, which are the reason for the changes in the Auger decay rates when $3d$ collapses,[18] are not limited to acting within a configuration but interactions of the same form connect doublet terms in different configurations.[30] Already, Minnhagen[17] noted that there appears to be a repulsion between $(^1S)3d\ ^2D$ and $(^3P)4d\ ^2D$ since the $(^1S)3d\ ^2D$ term appears to lie too low and the $(^3P)4d\ ^2D$ term too high. This interaction is also the reason for the two-step autoionization process since it, in addition, connects, for example, bound $(^1S)nd\ ^2D$ terms with continuum $(^3P)\epsilon d\ ^2D$ states. Similarly it will contribute to shake-up and -down processes but we have not included it here since our final states include only one d configuration. We believe, however, that there are experimental indications that the process is significant and responsible for most of the remaining discrepancies between theory and observations as discussed later.

The calculations were carried out using the suite of programs written by Cowan.[31] In Ca we did not use scaling of the electrostatic integrals, this leads to a too large energy splitting of the configurations,[18,31] but did not lead to drastic deviations between experiment and theory with regard to decay rates. However, in the case of Ar we noticed a clear discrepancy between calculated decay rates and experiment for the $3p^43d$ final configuration. Thus we have applied scaling for this configuration. In general, scaling is supposed to take neglected interactions from higher-lying configurations into account[32] but in this case it is probably more an indication of the fact that the calculated $3d$ collapse is too strong.

From the known $3p^44s$ and, in particular, $5s$ configuration it is possible to determine the scaling of $F^2(3p,3p)$, which is necessary in order to reproduce the $3p^4$ parent intervals reasonably well (85%). If this scaling is introduced [for $F^2(3p,3p)$] in $3p^43d$ it is found that the higher binding energy ^2D and ^2P terms still have much higher binding energies than determined experimentally.[17] These are the terms that have nondiagonal electrostatic matrix elements connecting them with the lower binding energy terms of the same type. Thus we can conclude that the $3p$-$3d$ electrostatic integrals need to be scaled down also. By scaling the exchange integrals down to 60% of the HF values we obtain a reasonable, although far from perfect, agreement with the observed energies. However, we do not expect to be able to obtain perfect agreement with the experimental energy separations because it is known that the interaction between series members of the p^4nd series in the rare gases must be included together with scaling in order to obtain good agreement.[30] Nevertheless, the scaling has important consequences for the mixing between, for example, the three ^2D terms (built on ^3P, ^1D, and ^1S). While in the *ab initio* calculation, the $(^3P)^2D$ term has the highest binding energy (if the largest eigenvector component is used to label the levels), when the 60% scaling is applied the ordering of the calculated energy levels using the same principle is closer to that in the $3p^4$ parent configuration (see Table II). There still is considerable mixing between the three basis states (we will in this paper use the labels given by Minnhagen[17] even though the $3p^4$ parent mixing sometimes gives other basis states as the dominant ones, see Table II and also Cowan[33]). In the *ab initio* calculation this mixing had the consequence that the largest decay rate from $2p^53d\ ^1P$ was to the highest $3p^43d\ ^2D$ term (Minnhagen ^1S) while the transition rate to the second ^2D term $[(^1D)^2D]$, which in a pure parent scheme, is the strongest, was much weaker. This,

TABLE II. Calculated Auger transition rates for the $2p^53d \rightarrow 2p^63p^4(3d+4s)$ transitions, the conventional "main lines" in units of 10^{10} sec^{-1}. The final ionic states are indicated according to the highest eigenvector component and according to the label used by Minnhagen (Ref. 17). To obtain the actual decay rates all numbers must be multiplied by the branching ratio in Table I, i.e., the numbers given are in fact relative. The contribution labeled p is due to the continuum p wave while the contribution labeled $p+f$ is the sum of the p and f waves.

Ar II term assignment			$2p^53d$ $(J=1)$					
	This	E_B (eV)	^3P		^1P		^3D	
Ref. 17	work[a]	(Ref. 17)	p	$p+f$	p	$p+f$	p	$p+f$
$3p^4(^3P)3d\ ^4D$	same	32.19	4450	4450	183	183	991	991
^4F	same	33.45	343	344	1004	1006	1595	1596
^2P	$(^1D)^2P$	33.78	1692	1693	119	123	338	344
^4P	same	34.06	1584	1584	817	817	1612	1613
$(^1D)4s\ ^2D$	$(^1D/^3P)3d\ ^2D$	34.20	2003	2017	67	83	363	391
$(^3P)3d\ ^2F$	same	34.31	16	28	24	29	24	32
^2D	$(^1D)4s\ ^2D$	34.46	953	960	63	75	230	248
$(^1D)3d\ ^2G$	same	34.88	b	656	b	469	b	540
^2F	same	36.02	340	530	1020	1199	1540	1774
^2D	same	37.15	478	499	3204	3236	2362	2408
^2P	$(^3P)^2P$	37.40	728	734	2080	2086	2417	2433
$(^1S)3d\ ^2D$	same	38.05	806	806	2124	2124	2121	2121
$(^1D)3d\ ^2S$	same	38.58	480	c	149	c	210	c

[a]The notation $(^1D/^3P)$ means near to 50:50 mixing between levels built on the indicated parent terms.
[b]No p-wave contribution.
[c]No f-wave contribution.

however, did not agree with the observed decay rates where the middle peak clearly is the more prominent. In the scaled calculation where the mixing is reduced the order is reversed and the calculated decay rates agree much better with experiment. There has been some discussion about the reality of this parent mixing and experimental verification is rather difficult. Cowan[33] noticed that the mixing led to a rearrangement of the oscillator strengths of transitions, for example, to the ground state from the three ^2D terms, but quantitative measurements of intensities are difficult because it is necessary to know the population distribution. Schweinzer *et al.*[34] demonstrated that the mixing leads to certain charge-exchange processes becoming allowed in collisions between Ar^{2+} ions and, for example, Li($2s$) atoms. However, it was difficult to measure the actual mixing coefficients in this way. We believe that the present experiment allows the most sensitive determination of the mixing so far. One advantage is that we are measuring a branching ratio which means that the result is independent of initial population distribution. Thus the measurements show that the calculations overestimate the degree of collapse of the $3d$ orbital in the $3p^43d$ configuration while in Ca the collapse is much further advanced and the decay rates are in agreement with a very strong mixing. The same conclusion can be drawn from the calculated shake probabilities for Ar which as we will see appear to be somewhat overestimated: in other words having a smaller overlap between the initial and final d orbital than observed.

For the higher $3p^4nd$ configurations, where the exchange interaction is much smaller and likewise the parent mixing, we have not used scaling but in the use of the results we have used the experimental energy-level positions whenever possible. In the calculation of the $3d+4s+5s$ final states we have moved the average energies of the two s configurations to get the best agreement with the experimental energies (the displacements are less than 0.5 eV). This leads in the calculation to a strong mixing (in fact inversion compared with Minnhagen's assignments) of the $3p^4(^1D)4s\ ^2D$ and $3p^4(^3P)3d\ ^2D$ terms which are located close to each other. This mixing, which does not have very strong effects on the decay rates from the $2p^53d\ ^1P$ level, does lead to the prediction that both ^2D terms can be reached from both the $2p^54s$ and the $2p^53d$ initial states with a similar probability. We give in Tables II and III the calculated transition probabilities for the decay of the $2p^53d$ resonance to the final $2p^63p^43d$ and $2p^63p^44d$ configurations as well as to the $4s\ ^2D$ term mentioned above. The values shown are calculated with the $2p^53d \rightarrow 3p^43d$ Auger interaction integrals without taking nonorthogonalities into account as described above. The values are, therefore, only valid as relative values within the configurations and absolute values can be obtained by multiplying all values with the appropriate branching ratios from Table I. In order to show the relative importance of the f wave we give, in the two tables, the separate contribution from the p wave as well as the total contribution from both types of continuum electrons. In order to show the effect of the f wave as accurately as possible, we have given the calculated transition rates with more decimals than warranted by the accuracy of the calculations which probably is not better than 10% and in some cases clearly worse. The initial $J=1$ levels are labeled by their largest LS component. In the observed spectrum where the large spin-orbit interaction for the $2p$ electron leads to a coupling which is far from LS, the unresolved levels labeled ^3P and ^1P belong to the series going to the lowest limit $2p^5\ ^2P_{3/2}$

TABLE III. Calculated Auger transition rates for the $2p^53d \rightarrow 2p^63p^44d$ transitions, the conventional "shake-up satellite lines" in units of 10^{10} sec^{-1}. The final ionic states are indicated according to the highest eigenvector component which agrees with the label used by Minnhagen (Ref. 17). To obtain the actual decay rates all numbers must be multiplied by the branching ratio in Table I, i.e., the numbers given are in fact relative. The contribution labeled p is due to the continuum p wave while the contribution labeled $p+f$ is the sum of the p and f waves.

Ar II term assignment			$2p^53d$ $(J=1)$					
	This	E_B (eV)	^3P		^1P		^3D	
Ref. 17	work	(Ref. 17)	p	$p+f$	p	$p+f$	p	$p+f$
$3p^4(^3P)4d\ ^4D$	same	38.55	4709	4709	155	156	865	865
^4F	same	38.77	156	157	1228	1229	1866	1867
^4P	same	38.90	1613	1613	872	872	1365	1365
^2F	same	38.96	54	55	95	96	18	18
^2P	same	39.36	1129	1130	533	534	272	275
^2D	same	39.64	997	1001	1486	1490	1543	1550
$(^1D)4d\ ^2G$	same	40.38	a	663	a	469	a	542
^2P	same	40.50	1815	1820	1913	1923	1997	2016
^2D	same	40.53	1403	1448	2407	2466	2665	2764
^2F	same	40.58	238	428	975	1156	1380	1606
^2S	same	41.21	818	b	397	b	410	b
	$(^1S)4d\ ^2D$	42.8[c]	1295	1295	1279	1279	1663	1663

[a]No p-wave contribution.
[b]No f-wave contribution.
[c]Value determined in this work.

and the level labeled ^3D goes to the upper limit. We have calculated that for the $2p_{3/2} \rightarrow 3d$ excitation the ^1P level is preferred to such an extent that in the comparison between the calculated Auger rates and observation we need not consider the decay of the ^3P level.

Recently Pan and Kelly[29] have published a calculation of the single- and double-photoionization cross sections in Ar including Auger effects with emphasis on the energy region below the $2p$ resonances. The rationale for the calculation was the measurements by Holland *et al.*[35] of the yields of multiply charged ions which showed a relatively sharp increase in the ratio between the yields of doubly and singly charged ions at about 220 eV, thus about 25 eV below the lowest $2p$ resonance. Pan and Kelly give double-photoionization cross sections for some of the lowest resonances, but without details of the individual Auger decay rates, and they point out that their results are less accurate in this region than below the resonance region. Our calculation is, therefore, complementing that of Pan and Kelly by being concerned with the actual Auger rates for the lowest resonances.

IV. RESULTS AND DISCUSSION

Figure 1(a) displays the electron spectrum for Ar recorded at a photon energy of $\hbar\omega = 246.9$ eV, i.e., the Ar* $2p^5(^2P_{3/2})3s^2 3p^6 3d$ resonance energy.[10] In addition to the $3s3p^6\ ^2S$ photoline at 217.7 eV kinetic energy

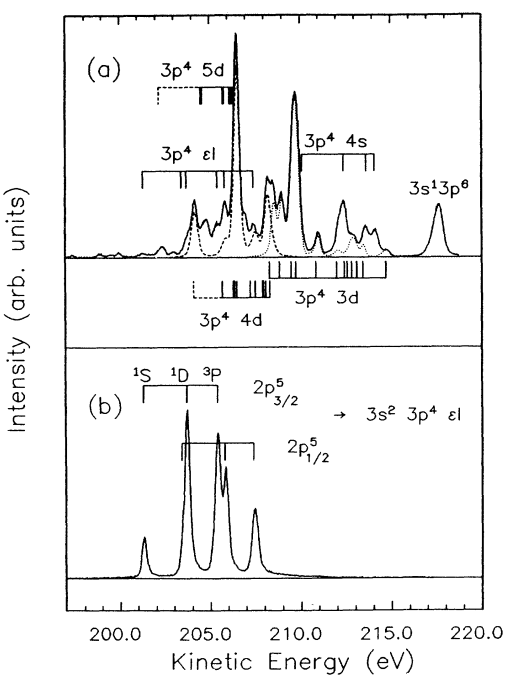

FIG. 1. (a) Electron spectrum of atomic Ar photoexcited at the Ar* $2p^5(^2P_{3/2})3s^2 3p^6 3d$ resonance ($\hbar\omega = 246.9$ eV) (solid curve). The $2p^5 3d \rightarrow 3p^4 3d\epsilon l$ (dotted curve) and $2p^5 3d \rightarrow 3p^4 4d\epsilon l$ (dashed curve) are experimental autoionization spectra obtained by the partitioning procedure described in the text. The line positions are derived from the binding energies given by Minnhagen (Ref. 17) and indicated by the vertical bars. (b) Ar $L_{23}M_{23}M_{23}$ Auger spectrum excited at $\hbar\omega = 270$ eV.

[binding energy 29.24 eV (Ref. 17)] strong autoionization lines are present in the range of kinetic energies between 202 and 216 eV. From optical data Minnhagen[17] derived the energy levels of the $3p^4 ns$ and $3p^4 nd$ configurations up to binding energies of 42.4 eV; the energy positions of the $2p^5 3d \rightarrow 3p^4 ns, nd$ autoionization lines derived from these data are indicated in Fig. 1(a). Note that, as mentioned, the structure of the Ar^+ $3p^4 3d$ configuration differs markedly from that of the Ar^{2+} $3p^4$ configuration due to the strength of the $3p$-$3d$ interaction. In the spectator model, the Auger spectrum would look similar to the spectrum following the decay of the $2p$ hole. However, as in the case of Ca (Ref. 18), the collapse of the $3d$ orbital and the resulting large $3p$-$3d$ interaction leads to an Auger spectrum which bears no resemblance to the $L_{23}M_{23}M_{23}$ Auger spectrum displayed in Fig. 1(b). Minnhagen[17] does not give binding energies for the Ar^+ $3p^4(^1S)4d, 5d\ ^2D$ states. However, we tentatively assign the lines at $E_{kin} = 204.1$ and 202.2 eV to transitions to $3p^4(^1S)4d\ ^2D$ and $3p^4(^1S)5d\ ^2D$ states, respectively, assuming the energy separation between the $3p^4(^1S)4d\,(5d)$ levels and the $3p^4(^1D)4d\,(5d)$ levels to be similar to that between the Ar^{2+} $3p^4(^1S)$ and $3p^4(^1D)$ parent terms; this is a reasonable approximation because the $4d$ and $5d$ electrons have a much smaller interaction with $3p$ than is the case for $3d$.

Due to the monochromator bandpass of about 0.6 eV the Ar* $2p^5(^2P_{1/2})3s^2 3p^6 4s$ resonance at $\hbar\omega = 246.5$ eV is excited to some degree when the monochromator is set to $\hbar\omega = 246.9$ eV. Thus part of the structure in our spectrum between $E_{kin} = 212$ and 215 eV is due to Ar^+ $3p^4 4s$ final states. The positions of these lines are also given in Fig. 1(a). The relative amplitude and shape of the Ar* $2p^5(^2P_{1/2})3s^2 3p^6 4s \rightarrow Ar^+$ $2p^6 3s^2 3p^4 4s$ autoionization lines were determined by setting the monochromator to the $2p$-$4s$ resonance energy of 246.5 eV. Similarly at low kinetic energies there is a small contribution to the experimental spectrum from the $L_{23}M_{23}M_{23}$ "normal" Auger lines arising from second-order light of the monochromator. We determined the spectrum of these Auger lines separately at a photon energy of 270 eV. Both of these spectra were used in the unraveling of the experimental spectrum which was carried out as follows. We approximated the experimental spectrum by a superposition of Voigt profiles for $3d$ and $4d$ centered on the line positions and by the experimental $4s$ and normal Auger spectra obtained as described above. The Lorentzian component [full width at half maximum (FWHM) = 0.12 eV (Ref. 10)] of the Voigt profiles accounts for the natural linewidths of the d levels involved and the Gaussian component simulates the spectrometer function of the electron energy analyzer. The relative amplitudes of the $3d$ and $4d$ lines were then varied to achieve the best agreement with the experimental results, while only the overall strength of the $4s$ and the normal Auger spectrum was allowed to vary. The spectrum thus obtained for the transitions to the $3p^4 3d$ and $4d$ states is indicated in Fig. 1(a) by the dotted and dashed lines, respectively, while the $4s$ and the normal Auger spectra are shown in Fig. 2(a) by dashed and dotted lines, respectively. A good overall approximation to the experimental results was achieved

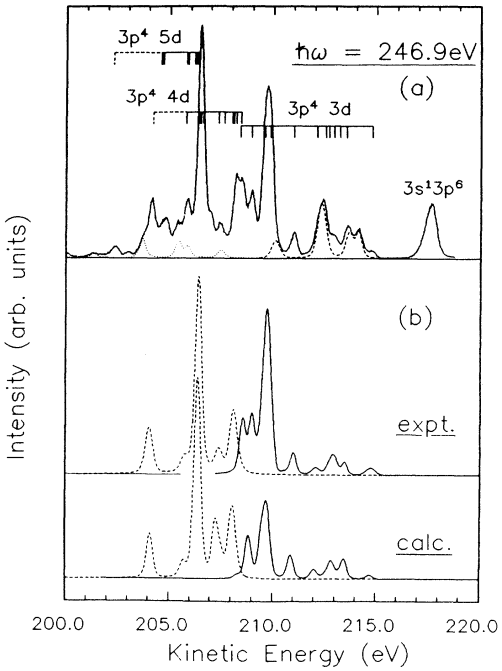

FIG. 2. (a) Experimental electron spectrum of atomic Ar photoexcited at the Ar* $2p^5(^2P_{3/2})3s^23p^63d$ resonance ($\hbar\omega=246.9$ eV) (solid line). $L_{23}M_{23}M_{23}$ Auger spectrum excited by the second-order light of the monochromator (dotted line). Ar* $2p^5(^2P_{1/2})3s^23p^64s \rightarrow Ar^+$ $2p^63s^23p^44s\epsilon l$ autoionization spectrum (dashed line). (b) Theoretical Ar* $2p^5(^2P_{3/2})3s^23p^63d \rightarrow Ar^+$ $2p^63s^23p^4nd\epsilon l$ ($n=3$ solid line, $n=4$ dashed line) autoionization spectra constructed from the calculated transition probabilities by a superposition of Voigt profiles (lower part) and the individual spectra extracted from the experimental intensity distributions as described in the text (upper part). The line positions are derived from the binding energies given by Minnhagen (Ref. 17) and marked by vertical bars in (a).

TABLE IV. Comparison between calculated relative transition probabilities (in %) for Ar* $2p^5(^2P_{3/2})3s^23p^63d$ "^1P" $\rightarrow Ar^+$ $2p^63s^23p^43d$ and observed values from the fit to the experimental spectrum described in the text. [*JK* coupling is the most appropriate coupling scheme for the $2p^53d$ configuration, but in agreement with standard practice we give the *LS* label (in quotation marks) together with the *J* value of the $2p^5$ core]. The results are given in the order of increasing binding energy. The term labels used are those chosen by Minnhagen (Ref. 17). Column 2 gives the experimental binding energies obtained from the fitting procedure (uncertainty ±0.3 eV).

Final-state assignments	Expt. E_B (eV)	Expt. I (%)	Calc. I (%)
$3p^4(^3P)3d\ ^4D$	32.2	2	2
$^4F+^2P$	33.5	5	10
$^4P+^2F+^2D+4s\ ^2D$	34.0	7	9
$(^1D)3d\ ^2G$	34.9	2	4
^2F	36.0	4	10
$^2D+^2P$	37.2	56	46
$(^1S)3d\ ^2D$	38.0	12	18
$(^1D)3d\ ^2S$	38.4	12	1

with some weak structures, which are accounted for in the fitting, ascribed to $3p^45s$ and $6s$ final states.

From the fitted spectrum we find a similar probability for the transitions from the $2p^53d$ resonance to the Ar^+ $3p^43d$ states and to the Ar^+ $3p^44d$ shake-up states while approximately 10% of the decays lead to Ar^+ $3p^45d$ shake-up states. The experimental branching ratios are summarized in Table I. The table shows that, summed over final states within a configuration, there is fairly good agreement with the calculated branching ratios (Table I). In order to see whether the agreement persists, when we consider the spectrum of individual lines within a configuration, we used the calculated branching ratios for the transitions Ar* $2p^53d \rightarrow Ar^+$ $3p^4nd$ ($n=3,4$) as well as the calculated transition probabilities for the transitions within each $3p^4nd$ configuration in order to synthesize a spectrum [Fig. 2(b)] by a superposition of Voigt profiles. (The energy values being taken from Minnhagen[17] where possible.) The FWHM of $\Gamma_{Voigt}=0.35$ eV is determined by the same parameters as discussed above. The comparison with the experimental spectrum [Fig. 2(a)] and, in particular, with the individual $3d$ and $4d$ spectra extracted from the experimental intensity distributions as described above [Fig. 2(b), upper part] clearly shows that the main features, i.e., the relative intensities of the different multiplets and the intensity distribution within these multiplets, are quite well reproduced by the calculations. The calculations overestimate the probability for shake-up transitions to Ar^+ $3p^44d$ states (see Table I), but the deviations from the experimental values are within the error limits of both the calculations and the experiment. Table IV shows the comparison between observed and calculated relative intensities within the $3d$ configuration, where the calculated values are summed over unresolved transitions expected to lie within the observed peaks. We see that there is, in general, good agreement between observed and calculated values although the calculated results for the $(^1D)^2F$ and ^2G terms indicate that the influence of the f wave is overestimated. The rather large discrepancy for the $(^1D)^2S$ term was expected since, as mentioned earlier, the two configuration approximation to the ^2S eigenvector is inadequate.[28] The remaining discrepancies concern the high ^2D and ^2P terms, which we expect to be mixed with the low ^2D and ^2P terms in $3p^44d$. As we will see, these are precisely the terms in $3p^44d$ for which the largest deviations are found.

The high probability for the Ar* $2p^53d \rightarrow Ar^+$ $3p^44d$ shake-up transitions has been discussed earlier[3,16] and has been ascribed to the collapse of the $3d$ wave function in the Ar^+ $3p^43d$ final state compared with the situation in the case of the initial $2p$ hole state. This finding is corroborated by our results. Another consequence of this collapse is the strong coupling between the $3p$ and $3d$ electrons, which leads to a spectrum which bears no resemblance to the $L_{23}M_{23}M_{23}$ Auger spectrum, as discussed already. Also the Ar* $2p^53d \rightarrow Ar^+$ $3p^44d$ autoionization spectrum differs markedly from the $L_{23}M_{23}M_{23}$ Auger spectrum. This shows that also for the Ar^+ $3p^44d$ states the *p-d* interaction cannot be neglected. Table V shows a comparison of observed and calculated relative

TABLE V. Comparison between calculated relative transition probabilities (in %) for Ar* $2p^5(^2P_{3/2})3s^23p^63d'$ "^1P" $\rightarrow$Ar$^+$ $2p^63s^23p^44d$ and observed values from the fit to the experimental spectrum described in the text. Column 2 gives the experimental binding energies obtained from the fitting procedure (uncertainty ±0.3 eV).

Final-state assignments	Expt. E_B (eV)	Expt. I (%)	Calc. I (%)
$3p^4(^3P)4d\ ^4D$	38.4	2	1
$^4F+{}^4P+{}^2F$	38.7	19	18
$^2P+{}^2D$	39.4	7	17
$(^1D)4d\ ^2G+{}^2P+{}^2D+{}^2F$	40.4	53	50
^2S	41.1	4	3
$(^1S)4d\ ^2D$	42.8	15	11

intensities for the observed transitions (satellites) in the $2p^53d\rightarrow 3p^44d$ system. The agreement is very satisfactory except for the unresolved ^2D plus ^2P terms for which we expect to have mixing with $3p^43d$ as already mentioned. Since $2p^53d$ decays to both $3p^43d$ and $3p^44d$ with similar probabilities, the decay rates to mixed terms will depend on branching ratios as well as phases in such a way that simple estimates of the rates are difficult.

The remaining discrepancies between the experimental and the theoretical spectrum (Fig. 2) are probably due to Ar* $2p^53d\rightarrow$Ar$^+$ $3p^4nd$ ($n>5$) shake-up decays and to transitions to $3p^4ns$ ($n>4$) states. Ar* $2p^54s\rightarrow$Ar$^+$ $3p^4ns$ shake-up transitions may also contribute because, as discussed above, the Ar* $2p^5(^2P_{1/2})4s$ resonance is excited to some extent. The 4s-5s shake-up prob-

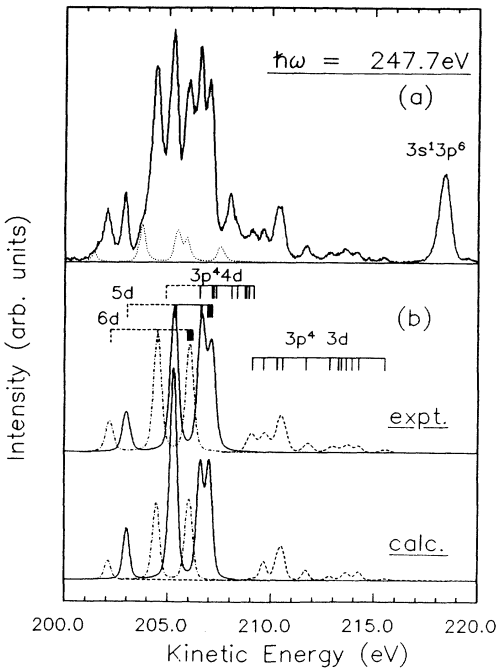

FIG. 3. (a) Experimental electron spectrum of atomic Ar photoexcited at the Ar* $2p^5(^2P_{3/2})3s^23p^64d$ resonance ($\hbar\omega$=247.7 eV) (solid line). $L_{23}M_{23}M_{23}$ Auger spectrum excited by second-order light of the monochromator (dotted line). (b) Theoretical Ar*$2p^5(^2P_{3/2})3s^23p^64d\rightarrow$Ar$^+$ $2p^63s^23p^4nd\epsilon l$ (n=3, dashed line; n=5, solid line; n=6, dash-dotted line) autoionization spectra constructed from the calculated transition probabilities by a superposition of Voigt profiles (lower part) and the individual spectra extracted from the experimental intensity distributions as described in the text (upper part). The line positions are derived from the binding energies given by Minnhagen (Ref. 17) and marked by vertical bars.

TABLE VI. Calculated Auger transition rates for the $2p^54d\rightarrow 2p^63p^4(3d+4s)$ transitions, the conventional "shake-down satellites" in units of 10^{10} sec^{-1}. The final ionic states are indicated according to the highest eigenvector component and according to the label used by Minnhagen (Ref. 17). To obtain the actual decay rates all numbers must be multiplied by the branching ratio in Table I, i.e., the numbers given are in fact relative. The contribution labeled p is due to the continuum p wave while the contribution labeled $p+f$ is the sum of the p and f waves.

Ar II term assignment		$2p^54d$ (J=1)					
	This	^3P		^1P		^3D	
Ref. 17	work[a]	p	$p+f$	p	$p+f$	p	$p+f$
$3p^4(^3P)3d\ ^4D$	same	4415	4415	229	229	1012	1012
^4F	same	365	366	1224	1226	1610	1611
^2P	$(^1D)^2P$	1681	1682	139	144	346	352
^4P	same	1594	1594	999	999	1626	1627
$(^1D)4s\ ^2D$	$(^1D/^3P)3d\ ^2D$	1954	1968	72	92	365	393
$(^3P)3d\ ^2F$	same	18	29	29	35	24	32
^2D	$(^1D)4s\ ^2D$	979	987	85	99	237	255
$(^1D)3d\ ^2G$	same	b	640	b	571	b	536
^2F	same	164	352	1250	1467	1560	1791
^2D	same	475	496	4028	4067	2386	2432
^2P	$(^3P)^2P$	726	732	2729	2736	2470	2486
$(^1S)3d\ ^2D$	same	804	804	2732	2732	2153	2153
$(^1D)3d\ ^2S$	same	482	c	250	c	224	c

[a]The notation $(^1D/^3P)$ means near 50:50 mixing between levels built on the indicated parent terms.
[b]No p-wave contribution.
[c]No f-wave contribution.

TABLE VII. Calculated Auger transition rates for the $2p^54d \rightarrow 2p^63p^45d$ transitions, the conventional "shake-up satellites" in units of 10^{10} sec^{-1}. The final ionic states are indicated according to the highest eigenvector component which agrees with the label used by Minnhagen (Ref. 17). To obtain the actual decay rates all numbers must be multiplied by the branching ratio in Table I, i.e., the numbers given are in fact relative. The contribution labeled p is due to the continuum p wave while the contribution labeled $p+f$ is the sum of the p and f waves.

Ar II term assignment			$2p^54d$ $(J=1)$					
	This	E_B (eV)	^3P		^1P		^3D	
Ref. 17	work	(Ref. 17)	p	$p+f$	p	$p+f$	p	$p+f$
$3p^4(^3P)5d\ ^4D$	same	40.56	4299	4299	176	177	774	774
^4F	same	40.67	131	133	1924	1925	1734	1735
^4P	same	40.74	1428	1429	1196	1196	1108	1108
^2F	same	40.79	59	60	119	119	77	77
^2D	same	41.11	447	448	2129	2130	2313	2314
^2P	same	41.17	1086	1087	1141	1141	544	545
$(^1D)5d\ ^2G$	same	42.32	a	647	a	571	a	539
^2D	same	42.38	1868	1924	2026	2106	2600	2722
^2F	same	42.40	194	376	1200	1416	1290	1501
	$(^1D)^2P$		1988	1992	2041	2053	1620	1635
	$(^1D)^2S$	42.65[b]	900	c	598	c	490	c
	$(^1S)^2D$	44.7[d]	1384	1384	1487	1487	1643	1643

[a]No p-wave contribution.
[b]Hansen and Persson (Ref. 36).
[c]No f-wave contribution.
[d]Determined in this work.

ability has been shown to amount to about 15%.[3,16,20] Since the $2p^5(^2P_{3/2})5s$ resonance coincides with the $2p^5(^2P_{3/2})3d$ resonance[10] some intensity may also stem from Ar^* $2p^55s \rightarrow Ar^+$ $3p^45s$ decays. (The $2p$-$5s$ oscillator strength has been calculated to be about 5% of the $2p$-$3d$ oscillator strength.)

Tuning the photon energy to the $2p^5(^2P_{3/2})3s^23p^64d$ resonance at $\hbar\omega=247.7$ eV (Ref. 10), the electron spectrum displayed in Fig. 3(a) has been recorded. For reference the $3s$ photoline is included. The autoionization spectrum differs markedly from that shown in Figs. 1(a) and 2(a). The main intensity is concentrated in a series of

TABLE VIII. Calculated Auger transition rates for the $2p^54d \rightarrow 2p^63p^46d$ transitions, the conventional "shake-up satellites" in units of 10^{10} sec^{-1}. The final ionic states are indicated according to the highest eigenvector component which agrees with the label used by Minnhagen (Ref. 17). To obtain the actual decay rates all numbers must be multiplied by the branching ratio in Table I, i.e., the numbers given are in fact relative. The contribution labeled p is due to the continuum p wave while the contribution labeled $p+f$ is the sum of the p and f waves.

Ar II term assignment			$2p^54d$ $(J=1)$					
	This	E_B (eV)	^3P		^1P		^3D	
Ref. 17	work	(Ref. 17)	p	$p+f$	p	$p+f$	p	$p+f$
$3p^4(^3P)6d\ ^4D$	same	41.52	4839	4839	481	482	1100	1101
^4F	same	41.59	103	103	2693	2694	1067	1067
^4P	same	41.67	1210	1210	1296	1296	685	685
^2F	same	41.69	44	45	57	57	807	808
^2P	same	41.75	1228	1228	975	975	873	873
^2D	same	41.77	349	350	1676	1676	2343	2343
	$(^1D)^2G$		a	647	a	571	a	538
	$(^1D)^2F$		160	338	1220	1435	1230	1433
	$(^1D)^2D$		1987	2048	1773	1856	2553	2685
	$(^1D)^2P$		2042	2046	1890	1902	1529	1544
	$(^1D)^2S$	43.41[b]	923	c	627	c	510	c
	$(^1S)^2D$	45.5[d]	1414	1414	1459	1459	1631	1631

[a]No p-wave contribution.
[b]Hansen and Persson (Ref. 36).
[c]No f-wave contribution.
[d]Determined in this work.

strong lines spanning an energy range of approximately 4 eV. As described above for the $2p^5 3d$ resonance we tried also here to separate the contributions from the different $2p^5 4d \rightarrow 3p^4 nd$ decay channels. Similarly, the $L_{23}M_{23}M_{23}$ Auger lines originating from ionization by second-order light were taken into account. The relative strengths obtained for the decay channels in this way are also presented in Table I. Ar* $2p^5 4d \rightarrow Ar^+$ $3p^4 nd$ ($n > 4$) shake-up transitions are found to make up more than 70% of the total intensity. Approximately 10% of the intensity is due to shake-down processes, leaving the Ar^+ ion in the $3p^4 3d$ state. The most striking result is that the $2p^5 4d \rightarrow 3p^4 4d$ decay (the main line) is strongly suppressed. An upper limit of 15% has been obtained by ascribing the maxima at 209.2 and at 208.1 eV and the major part of the maximum at 207.1 eV to the $2p^5 4d \rightarrow 3p^4 4d$ channel. Actually, for the peak at 207.1 eV our calculations ascribe the dominant contribution to the $2p^5 4d \rightarrow 3p^4 5d$ decay. Of the lines assigned to $2p^5 4d \rightarrow 3p^4 4d$, the 207.1 eV and the strong 208.1 eV peaks both have ^2D or ^2P character and, in particular, the strength of the 208.1 eV peak could be due, in part, to the mixing with $3d$ and $5d$ described earlier. In this sense the 15% upper limit on the $4d \rightarrow 4d$ decay is a real upper limit insofar as the series interaction in this case appears to partially cancel the shake-up probability. We do not believe that this effect has been observed before. In terms of the simple shake model the 15% upper limit means that the $4d$ wave function in the excited Ar* $2p^5 4d$ state and the final Ar^+ $3p^4 4d$ state are almost orthogonal. The calculated $2p^5 4d \rightarrow 3p^4 nd$ transition probabilities given in Table I agree with the experimental values. In particular, the $2p^5 4d \rightarrow 3p^4 4d$ decay is calculated to be "forbidden," only 0.04% of the decays being predicted to go to the Ar^+ $3p^4$ $4d$ states. As mentioned earlier, the calculations seem to overestimate the degree of collapse although the neglected d series mixing is a source of uncertainty. The theoretical $2p^5 4d \rightarrow 3p^4 nd$ autoionization spectrum synthetized in the same way as described for the decay of the $2p^5 3d$ resonance and the individual $3d$, $5d$, and $6d$ spectra extracted from the experimental intensity distributions, as described above, are presented in Fig. 3(b). The energy positions of the autoionization lines obtained from Minnhagen[17] are indicated. The main features of the experimental spectrum are again well reproduced by the calculated spectrum. The latter seems to overestimate the $2p^5 4d \rightarrow 3p^4 5d$ channel and underestimate the $2p^5 4d \rightarrow 3p^4 6d$ channel. However, part of these discrepancies may be due to the limited energy resolution of the monochromator because the $2p^5(^2P_{3/2})5d$ resonance ($\hbar\omega = 248.0$ eV) is also excited to some degree when the monochromator is tuned to the $2p^5(^2P_{3/2})4d$ resonance. This results in a reduction of the intensity of the $2p^5 4d \rightarrow 3p^4 5d$ decays and an enhancement of the intensity of decays to $3p^4 6d$ final states. Tables VI, VII, and VIII give the calculated Auger transition rates for the $2p^5 4d \rightarrow 2p^6 3p^4(3d + 4s)$, $5d$, and $6d$ transitions again with more decimals than warranted by the expected accuracy of the calculations. The comparison between the calculated relative transition probabilities for the $2p^5(^2P_{3/2})4d \rightarrow 3p^4 nd$ decay ($n = 3,5,6$) and the experimental values are presented in Tables IX–XI. There is good agreement between both sets of data except for the $3p^4(^1D)3d\ ^2S$ and $3p^4(^1D)3d\ ^2D + ^2P$ final states where we encounter similar discrepancies as for the decay of the $2p^5 3d$ resonance (see Table IV).

TABLE IX. Comparison between calculated relative transition probabilities (in %) for Ar* $2p^5(^2P_{3/2})3s^2 3p^6 4d$ "^1P" $\rightarrow Ar^+$ $2p^6 3s^2 3p^4 3d$ and observed values from the fit to the experimental spectrum described in the text. The term labels used are those given by Minnhagen (Ref. 17). Column 2 gives the experimental binding energies obtained from the fitting procedure (uncertainty ±0.3 eV).

Final-state assignments	Expt. E_B (eV)	Expt. I (%)	Calc. I (%)
$3p^4(^3P)3d\ ^4D$	32.1	2	2
$^4F + ^2P$	33.4	4	9
$^4P + ^2P + ^2D + 4s\ ^2D$	34.0	7	8
$(^1D)3d\ ^2G$	34.7	9	4
^2F	35.9	8	10
$^2D + ^2P$	37.2	34	46
$(^1S)3d\ ^2D$	37.9	18	19
$(^1D)3d\ ^2S$	38.6	18	2

TABLE X. Comparison between calculated relative transition probabilities (in %) for Ar* $2p^5(^2P_{3/2})3s^2 3p^6 4d$ "^1P" $\rightarrow Ar^+$ $2p^6 3s^2 3p^5 5d$ and observed values from the fit to the experimental spectrum described in the text. Column 2 gives the experimental binding energies obtained from the fitting procedure (uncertainty ±0.3 eV).

Final-state assignments	Expt. E_B (eV)	Expt. I (%)	Calc. I (%)
$3p^4(^3P)5d\ ^4D + ^4F + ^4P + ^2F$	40.6	24	23
$^2D + ^2P$	41.1	31	22
$(^1D)5d\ ^2G + ^2D + ^2F + ^2P + ^2S$	42.4	35	45
$(^1S)5d\ ^2D$	44.7	10	10

V. CONCLUSIONS

We also calculated the relative probabilities for the decay of the $2p^5 5d$ and $2p^5 6d$ resonances into $3p^4 nd$ ($n = 3,4,5,6,7,8,9$) states. As for the decay of the $2p^5 3d$ and $2p^5 4d$ resonances we find a strong dependence on the

TABLE XI. Comparison between calculated relative transition probabilities (in %) for Ar* $2p^5(^2P_{3/2})3s^2 3p^6 4d$ "^1P" $\rightarrow Ar^+$ $2p^6 3s^2 3p^4 6d$ and observed values from the fit to the experimental spectrum described in the text. Column 2 gives the experimental binding energies obtained from the fitting procedure (uncertainty ±0.3 eV).

Final-state assignments	Expt. E_B (eV)	Expt. I (%)	Calc. I (%)
$3p^4(^3P)6d\ ^4D + ^4F + ^4P + ^2F + ^2P + ^2D$	41.6	42	48
$(^1D)6d\ ^2G + ^2F + ^2D + ^2P + ^2S$	43.2	46	43
$(^1S)6d\ ^2D$	45.5	12	10

principal quantum number n. The results are summarized in Table I. Due to the limited resolution of the monochromator, the decay of the $2p^5nd$ resonances ($n>4$) could not be studied experimentally. However, there are two important results which directly can be read off from Table I.

(i) The total shake probability, i.e., shake-down plus shake-up, increases from the $2p^53d$ resonance to the $2p^56d$ resonance. Our total shake probabilities are close to the values estimated (using, however, basically the same computer program) by Heimann *et al.*[4] for the sum of shake-up and shake-off processes. Their values are roughly equal to 1 minus the "diagonal" values in Table I: the probability for the main line. The largest difference is found for the $3d$ resonance where we predict $3d\rightarrow 3d$ to be 32% while Heimann *et al.* give 22%. Our value is closer to experiment (42%). However, while Heimann *et al.* conclude that shake-off is much more important than shake-up, the shake-up process dominates the $2p^5nd$ resonances studied by us for $n<6$ and far exceed the shake-off decays. This favors the two-step decay of the resonances proposed by Hayaishi *et al.*[8,19] as the main cause of the Ar^{2+} ions below the $2p$ thresholds. Heimann *et al.* mention that, at least for Xe, they have calculated shake-up to be more important than shake-off, but they express doubt about the validity of this result, which disagreed with their conclusions about the greater importance of shake-off. However, our experimental results confirm, as discussed already, the calculated shake-up rates (for Ar) to a high accuracy and indicate that the calculations, at least for Ar, are reliable. Also Pan and Kelly[29] commented on the results of Heimann *et al.*[4] and noted a considerable increase in their own calculated double-photoionization cross section relative to the single-photoionization cross section in the resonance region. However, their calculation (see Fig. 8 of their paper) also seems to predict an increase with n which does not agree with the maximum in the region of $n=6$, which was observed experimentally by Hayaishi *et al.*[19] and Heimann *et al.*[4] Thus, the calculations by Pan and Kelly[29] also seem to lead to the conclusion that two-step autoionization is the stronger effect at low n. It should be pointed out that it is a condition for the validity of the two-step autoionization model in this case, that shake-up from $4s$ and $3d$ is limited to states below the $3p^4\,{}^3P$ thresholds, thus, for example, if there is a $3d\rightarrow 6d$ shake-up probability, there should be a commensurate intensity of threshold electrons connected with the $3d$ photon resonance energy. The very small intensity of threshold electrons actually observed at this resonance[4,19] is in agreement with the fact that we do not find evidence for a $3d\rightarrow 6d$ shake-up process. The situation for resonant production of threshold electrons in Kr $3d$ and Xe $4d$ excitation appears to be rather different from that in Ar. In particular, in Kr and Xe the resonant threshold electron production appears to increase with n contrary to the situation in Ar.

(ii) The probability for the $2p^5nd\rightarrow 3p^4nd$ decay is low for $n=5,6$ after having reached the minimum for $n=4$ and the overlap between the nd states in the $2p$ core excited state and the final ion state remains very small. In these circumstances the familiar method of determining the nature of the core excited state or the final state of the ion by looking for the resonant enhancement of an autoionization line can be expected to fail, because it is based on the assumption that the dominant decay process leaves the principal quantum number and the angular momentum of the excited electron unchanged.

In conclusion, the present experiment seems to give the clearest information obtained so far about the degree of collapse of the $3d$ orbital in Ar II. In doing so it has shown the reality of the $3p^4$ parent mixing due to the strength of the $3p$-d interaction both within and between configurations.

ACKNOWLEDGMENTS

The authors are especially indebted to C. Kunz, S. Cramm, and I. Storjohann for being able to use the FLIPPER I station and for their help in operating it. The continuous support of the HASYLAB staff is gratefully acknowledged. This work was supported by the Bundesministerium für Forschung und Technologie der Bundesrepublik Deutschland. The calculations were performed on the CYBER 205 computer in Amsterdam under Grant No. SC-20 from the Cooperative Body for Advancement of Computer Services in Higher Education and Scientific Research (SURF).

[1] H. Aksela, S. Aksela, H. Pulkkinen, G. M. Bancroft, and K. H. Tan, Phys. Rev. A **33**, 3876 (1986).

[2] H. Aksela, S. Aksela, G. M. Bancroft, K. H. Tan, and H. Pulkkinen, Phys. Rev. A **33**, 3867 (1986).

[3] H. Aksela, S. Aksela, H. Pulkkinen, G. M. Bancroft, and K. H. Tan, Phys. Rev. A **37**, 1798 (1988).

[4] P. A. Heimann, D. W. Lindle, T. A. Ferrett, S. H. Liu, L. J. Medhurst, M. N. Piancastelli, D. A. Shirley, U. Becker, H. G. Kerkhoff, B. Langer, D. Szostak, and R. Wehlitz, J. Phys. B **20**, 5005 (1987).

[5] T. A. Carlson, D. R. Mullins, C. E. Beall, B. W. Yates, J. W. Taylor, D. W. Lindle, and F. A. Grimm, Phys. Rev. A **39**, 1170 (1989).

[6] J. W. Cooper, Phys. Rev. A **39**, 3714 (1989).

[7] M. Nakamura, M. Sasanuma, S. Sato, M. Watanabe, H. Yamashita, Y. Iguchi, A. Ejiri, S. Nakai, S. Yamaguchi, T. Sagawa, Y. Nakai, and T. Oshio, Phys. Rev. Lett. **21**, 1303 (1968).

[8] T. Hayaishi, Y. Morioka, Y. Kageyama, M. Watanabe, I. H. Suzuki, A. Mikuni, G. Isoyama, S. Asaoka, and M. Nakamura, J. Phys. B **17**, 3511 (1984).

[9] G. C. King, M. Tronc, F. H. Read, and R. C. Bradford, J. Phys. B **10**, 2479 (1977).

[10] G. C. King and F. H. Read, in *Atomic Inner-Shell Physics*, edited by B. Crasemann (Plenum, New York, 1985), p. 317.

[11] W. Mehlhorn and D. Stalherm, Z. Physik **217**, 294 (1968).

[12] L. O. Werme, T. Bergmark, and K. Siegbahn, Phys. Scr. **8**, 149 (1973).

[13]E. J. McGuire, Phys. Rev. A **11**, 1880 (1975).
[14]K. G. Dyall and F. P. Larkins, J. Phys. B **15**, 2793 (1982).
[15]J. E. Hansen and W. Persson, J. Phys. B **20**, 693 (1987).
[16]H. Aksela, S. Aksela, H. Pulkkinen, A. Kivimäki, and O.-P. Sairanen, Phys. Scr. **41**, 425 (1990).
[17]L. Minnhagen, Ark. Fys. **25**, 203 (1963).
[18]M. Meyer, E. v. Raven, M. Richter, B. Sonntag, R. D. Cowan, and J. E. Hansen, Phys. Rev. A **39**, 4319 (1989).
[19]T. Hayaishi, E. Murakami, A. Yagishita, F. Koike, Y. Morioka, and J. E. Hansen, J. Phys. B **21**, 3203 (1988).
[20]M. Meyer, E. v. Raven, M. Richter, B. Sonntag, and J. E. Hansen, in *Proceedings of the Fourth International Conference on Electron Spectroscopy, Hawaii, 1989* [J. Electron Spectrosc. **51**, 407 (1990)].
[21]M. Meyer, E. v. Raven, B. Sonntag, and J. E. Hansen, in *Proceedings of the Second European Conference on Progress in X-ray Synchrotron Radiation Research, Rome, 1989,* edited by A. Balerna, E. Bernieri, and S. Mobilio (Italian Physical Society, Bologna, 1990), Vol. 25.
[22]F. Senf, K. Behrens v. Rautenfeld, S. Cramm, C. Kunz, J. Lamp, V. Saile, J. Schmidt-May, and J. Voss, Nucl. Instrum. Methods A **246**, 314 (1986).
[23]T. Åberg, Ann. Acad. Sci. Fenn. Ser. A **6**, 308 (1969).
[24]R. L. Martin and D. A. Shirley, Phys. Rev. A **13**, 1475 (1976).
[25]T. A. Carlson and M. O. Krause, Phys. Rev. Lett. **17**, 1079 (1966).
[26]R. D. Cowan and D. C. Griffin, J. Opt. Soc. Am. **66**, 1010 (1976).
[27]J. E. Hansen, J. Phys. B **5**, 1083 (1972).
[28]H. Smid and J. E. Hansen, J. Phys. B **16**, 3339 (1983).
[29]Ch. Pan and H. P. Kelly, Phys. Rev. A **39**, 6232 (1989).
[30]J. E. Hansen and W. Persson, Phys. Scr. **36**, 602 (1987).
[31]R. D. Cowan, *The Theory of Atomic Structure and Spectra* (California University Press, Berkeley, 1981), Chaps. 8 and 16.
[32]B. G. Wybourne, *Spectroscopic Properties of Rare Earths* (Interscience, New York, 1965), Sec. 2–17.
[33]R. D. Cowan, J. Opt. Soc. Am. **58**, 924 (1968).
[34]J. Schweinzer, U. Jellen-Wutte, W. Vanek, H. Winter, and J. E. Hansen, J. Phys. B **21**, 315 (1988).
[35]D. P. M. Holland, K. Codling, J. B. West, and G. V. Marr, J. Phys. B **12**, 2465 (1979).
[36]J. E. Hansen and W. Persson, J. Phys. B **15**, L269 (1982).